PAPER

Low Grazing Scattering from Sinusoidal Neumann Surface with Finite Extent: Total Scattering Cross Section

Junichi NAKAYAMA[†a] *and* **Yasuhiko TAMURA**[†], *Members*

SUMMARY　This paper deals with the scattering of a transverse magnetic (TM) plane wave from a perfectly conductive sinusoidal surface with finite extent. By use of the undersampling approximation and a rectangular pulse approximation, an asymptotic formula for the total scattering cross section at a low grazing limit of incident angle is obtained explicitly under conditions such that the surface is small in roughness and slope, and the corrugation width is sufficiently large. The formula shows that the total scattering cross section is proportional to the square root of the corrugation width but does not depend on the surface period and surface roughness. When the corrugation width is not large, however, the scattered wave can be obtained by a single scattering approximation, which gives the total scattering cross section proportional to the corrugation width and the Rayleigh slope parameter. From the asymptotic formula and the single scattering solution, a transition point is defined explicitly. By comparison with numerical results, it is concluded that the asymptotic formula is fairly accurate when the corrugation width is much larger than the transition point.
key words:　scattering, finite periodic surface, TM wave, total scattering cross section, low grazing angle of incidence

1. Introduction

This paper deals with the scattering of a TM plane wave from a perfectly conductive sinusoidal surface with a finite corrugation width W (See Fig. 1). We study the total scattering cross section at a low grazing limit of incidence (LGLI) with $\theta_i \to 0$.

　　Low grazing angle scattering from a rough surface is practically important in the sea observation by a ground based high frequency (HF) radar [1]. However, the diffraction by a periodic surface often becomes singular at LGLI, at which no diffraction takes place and the reflection coefficient becomes -1. Such singular behavior is demonstrated analytically and numerically for a periodic Neumann surface with small roughness and gentle slope [2], [3] and for a periodic array of grooves with large groove depth [4]. However, it appears in several numerical works [5]–[7] as such phenomena that the 0th order diffraction efficiency becomes unity and any other order diffraction efficiencies vanish at LGLI.

　　On the other hand, it is predicted that the scattering must occur at LGLI, if the rough surface is finite in extent [8]. The prediction is supported numerically for a finite sinusoidal surface [9]–[11] and for a finite periodic array of rectangular grooves [12].
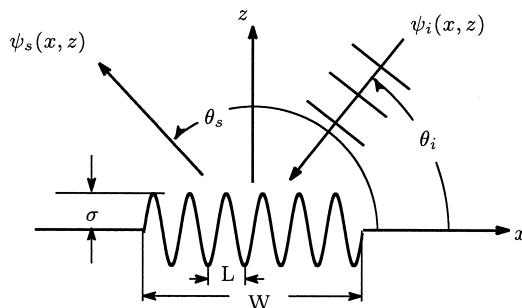
Fig. 1　The scattering of a TM plane wave from a periodic surface with finite extent. $\psi_i(x, z)$ and $\psi_s(x, z)$ are the incident plane wave and the scattered wave, respectively. θ_i and θ_s are the angle of incidence and a scattering angle, respectively. W and σ are the width and roughness of the corrugation, respectively.

Such a gap between a finite and infinite periodic cases may be solved, if we obtain the asymptotic behavior of the total scattering cross section at LGLI as $W \to \infty$. This is because a finite periodic surface approaches to a periodic surface as $W \to \infty$. Taking this idea, we numerically calculated the total scattering cross section against the corrugation width for two cases: a finite periodic array of rectangular grooves [12] and a finite sinusoidal surface [11]. From numerical results, we estimated that the total scattering cross section must diverge but the total scattering cross section per unit surface must vanish at LGLI as the corrugation width goes to infinity. However, it is essentially difficult to obtain by a numerical method the asymptotic behavior of the total scattering cross section. However, analytical theories have not been developed yet.

　　This paper obtains an asymptotic formula of the total scattering cross section at LGLI. We start with the undersampling approximation [10], [11], where the angular spectrum of the scattered wave is approximately represented by a finite undersampling sequence. We derive a matrix equation for the finite sequence and then evaluate analytically the matrix elements given by integrals by use of a rectangular pulse approximation. In general, the matrix equation cannot be solved analytically. In a special case where the angle of incidence becomes low grazing and W is sufficiently large, we obtain an analytic expression of the 0th component of the finite sequence by Cramer's formula, in terms of which a new asymptotic formula for the total scattering cross section at LGLI is obtained. The formula represents a remarkable fact that the total scattering cross section is independent of the period and the surface roughness and increases

in proportion to the square root of the corrugation width. By comparison with numerical results, it is then shown that the asymptotic formula is fairly accurate when the corrugation width is large enough.

Next, we consider a case where the corrugation is small in roughness and is not large in width. In such a case, the scattered wave can be obtained by a single scattering approximation [13], which gives the total scattering cross section proportional to the Rayleigh slope parameter and the corrugation width. From the asymptotic formula and the single scattering solution, a transition point W_t is defined explicitly. It is then shown numerically that the asymptotic formula becomes fairly accurate in the multiple scattering region where the corrugation width is much larger than the transition point.

In this paper, a time variation $e^{-i\omega t}$ is assumed and suppressed.

2. Formulation

We consider the scattering of a TM plane wave from a sinusoidal surface with finite extent shown in Fig. 1. We write the surface corrugation as

$$z = f(x) = \sigma u(x|W)\sin(k_L x), \quad k_L = \frac{2\pi}{L}, \quad (1)$$

$$u(x|W) = u^2(x|W) = \begin{cases} 1, & |x| \leq W/2 \\ 0, & |x| > W/2 \end{cases}, \quad (2)$$

where L is the period, k_L is the spatial angular frequency of the period L, and W is the width of corrugation which is an integer multiple of the period L to make $f(x)$ continuous at $x = \pm W/2$. $u(x|W)$ is a rectangular pulse, and σ is the surface roughness. We denote the y component of the magnetic field by $\psi(x, z)$, which satisfies

$$\left[\frac{\partial^2}{\partial x^2} + \frac{\partial^2}{\partial z^2} + k^2\right]\psi(x, z) = 0, \quad (3)$$

in the region $z > f(x)$ and the Neumann condition on the surface (1)

$$\left[\frac{\partial}{\partial z} - \frac{df}{dx}\frac{\partial}{\partial x}\right]\psi(x, z)\bigg|_{z=f(x)} = 0. \quad (4)$$

Here, $k = 2\pi/\lambda$ is wave number and λ is wavelength. We write the incident plane wave $\psi_i(x, z)$ as

$$\psi_i(x, z) = e^{-ipx}e^{-i\beta(p)z}, \quad p = k \cdot \cos\theta_i, \quad (5)$$

where θ_i is the angle of incidence (See Fig. 1) and $\beta(p)$ is a function of p defined by

$$\beta(p) = \sqrt{k^2 - p^2}, \quad Re\,[\beta(p)] \geq 0, \quad Im\,[\beta(p)] \geq 0. \quad (6)$$

Here, Re and Im are real and imaginary part, respectively. Since the surface is flat for $|x| > W/2$, we put

$$\psi(x, z) = \psi_i(x, z) + e^{-ipx}e^{i\beta(p)z} + \psi_s(x, z), \quad (7)$$

where the second term in the right-hand side is the specularly reflected wave and $\psi_s(x, z)$ is the scattered wave due to the surface corrugation. We write an approximate expression of $\psi_s(x, z)$ as

$$\psi_s(x, z) = \int_{-k_B}^{k_B} \frac{A_\beta(s)}{\beta(p+s)} e^{-i(p+s)x + i\beta(p+s)z}ds, \quad (8)$$

which is made up of up-going plane waves and evanescent waves. Here, k_B is a truncated band width and $A_\beta(s)$ is the angular spectrum, which is the amplitude of the partial wave scattered into the $\theta_s = \Theta(p + s)$ direction. Here, $\Theta(p + s)$ is defined by

$$\Theta(p + s) = \arccos\left[-\frac{p+s}{k}\right] = \int_{-(p+k)}^{s} \frac{ds'}{\beta(p+s')}, \quad (9)$$

which is complex in general. We note that $\Theta(k) = \pi$ and $\Theta(-k) = 0$. If we put $s = mk_L$, $(m = 0, \pm 1, \pm 2, \cdots)$, this becomes a famous grating formula [14] for a perfectly periodic surface,

$$\Theta(p + mk_L) = \arccos[-(p + mk_L)/k], \quad (10)$$

where $\Theta(p + mk_L)$ is the mth order diffraction angle. We assume that the scattered wave $\psi_s(x, z)$ satisfies the Sommerfeld radiation condition and becomes a cylindrical wave in the far region.

The optical theorem is analogous to the famous forward scattering theorem and may be written as [9],

$$p_c = p_{inc}, \quad (11)$$

$$p_c = -\frac{4\pi}{k}Re[A_\beta(0)], \quad (12)$$

$$p_{inc} = \frac{W}{2\pi}\int_0^\pi \sigma_s(\theta_s|\theta_i)d\theta_s, \quad (13)$$

$$\sigma_s(\theta_s|\theta_i) = \frac{4\pi^2}{kW}|A_\beta(-k\cos\theta_s - k\cos\theta_i)|^2. \quad (14)$$

Here, $\sigma_s(\theta_s|\theta_i)$ is the differential scattering cross section per unit surface. The optical theorem (11) states that the total scattering cross section p_{inc} is equal to p_c the loss of the amplitude of the partial wave scattered into the specularly reflection direction. Because of (11), however, we will call p_c the total scattering cross section.

2.1 Undersampling Approximation

For a sufficiently large W, let us calculate $A_\beta(s)$ by the undersampling approximation [10], [11], in which the scattered wave is physically approximated by a finite sum of beams diffracted into directions given by the grating formula (10) and effects of edges at $x = \pm W/2$ are neglected implicitly.

Let us write an undersampling approximation of the angular spectrum $A_\beta(s)$ as

$$A_\beta(s) = \frac{1}{2\pi}\sum_{n=-N_Q}^{N_Q} Q_n U(s - nk_L|W), \quad (15)$$

$$U(s|W) = \int_{-\infty}^{\infty} u(x|W)e^{isx}dx = \frac{\sin(sW/2)}{(s/2)}, \quad (16)$$

$$U(nk_L|W) = W\delta_{n,0}, \quad (17)$$

$$\lim_{W\to\infty} U(s|W) = 2\pi\delta(s), \quad (18)$$

where $[Q_n]$ is a finite undersampling sequence, $U(s|W)$ is the Fourier transform of $u(x|W)$, δ_{mn} is Kronecker's delta and $\delta(s)$ is Dirac's delta function. Physically, (15) represents a finite sum of diffraction beams, where Q_n is the amplitude of the nth order diffraction beam scattered into the $\theta_s = \Theta(p + nk_L)$ direction with a beam shape described by $U(s - nk_L|W)$.

Substituting (7) and (8) into (1), we obtain a set of equations for vector $[Q_l]$ after some manipulations,

$$\sum_{n=-N_Q}^{N_Q} D_{l,n}(p)Q_n = E_l(p), \quad (19)$$

$$D_{l,n}(p) = \sum_{m=-\infty}^{\infty} \int_{-k_B}^{k_B} \frac{C_m(p+s, \beta(p+s))}{2\pi W\beta(p+s)}$$
$$\times U(s - nk_L|W)U(s + (m-l)k_L|W)ds, \quad (20)$$

$$E_l(p) = -[C_l(p, -\beta(p)) + C_l(p, \beta(p))], \quad (21)$$

$$C_m(\alpha, \beta) = \beta J_{-m}(\sigma\beta)$$
$$+ \frac{\sigma\alpha k_L}{2}(J_{1-m}(\sigma\beta) + J_{-1-m}(\sigma\beta)), \quad (22)$$

where $J_m(\cdot)$ is the Bessel function. Here, (15), (16) and (17) were obtained in Ref. [10], where the integral in (20) was calculated numerically to solve (19). However, we will obtain an analytical expression of the integral in (20) for sufficiently large W.

2.2 Rectangular Pulse Approximation

To evaluate the integral in (20) analytically, we first rewrite (22) as

$$C_m(\alpha, \beta) = \frac{\sigma\alpha k_L}{2}(\delta_{m,1} + \delta_{m,-1}) + \beta v_m(\alpha, \beta),$$

$$v_m(\alpha, \beta) = J_{-m}(\sigma\beta) + \frac{\sigma\alpha k_L}{2}$$
$$\times \frac{J_{1-m}(\sigma\beta) - \delta_{m,1} + J_{-1-m}(\sigma\beta) - \delta_{m,-1}}{\beta}, \quad (23)$$

$$\lim_{\beta\to 0} v_m(\alpha, \beta) = \delta_{m,0}, \quad (24)$$

$$\lim_{\beta\to 0} C_m(\alpha, \beta) = \frac{\sigma\alpha k_L}{2}(\delta_{m,1} + \delta_{m,-1}). \quad (25)$$

Using these formulas, we may rewrite (20) as

$$D_{l,n}(p) = \sum_{m=\pm 1} \int_{-k_B}^{k_B} \frac{\sigma k_L(p+s)}{4\pi W\beta(p+s)}$$
$$\times U(s - nk_L|W)U(s + (m-l)k_L|W)ds$$
$$+ \sum_{m=-\infty}^{\infty} \int_{-k_B}^{k_B} \frac{v_m(p+s, \beta(p+s))}{2\pi W}$$
$$\times U(s - nk_L|W)U(s + (m-l)k_L|W)ds, \quad (26)$$

which is evaluated asymptotically below.

When $W \to \infty$, $U(s|W)$ becomes Dirac's delta function by (18). This suggests that $U(s|W)$ may be approximated by a narrow rectangular pulse if W is sufficiently large. Thus, we roughly approximate $U(s|W)$ as

$$U(s|W) \approx Wu(s|k_W), \quad k_W = \frac{2\pi}{W}, \quad (27)$$

which we call the rectangular pulse approximation. By (27), we have approximate formulas as follows.

$$\int_{-\infty}^{\infty} f(s)U(s - nk_L|W)U(s - mk_L|W)ds$$
$$\approx 2\pi W f(nk_L)\delta_{n,m}, \quad (28)$$

$$\int_{-\infty}^{\infty} \frac{f(s)U(s - nk_L|W)U(s - mk_L|W)}{\beta(p+s)}ds$$
$$\approx \frac{2\pi W}{k} f(nk_L)\delta_{n,m}\Delta(p + nk_L|W). \quad (29)$$

Here, $f(s)$ is a slowly varying continuous function and

$$\Delta(p, W) = \frac{k}{2\pi W} \int_{-\infty}^{\infty} \frac{U^2(s|W)}{\beta(p+s)}ds \quad (30)$$

$$\approx \frac{kW}{2\pi} \int_{-k_W/2}^{k_W/2} \frac{u^2(s|k_W)}{\beta(p+s)}ds \quad (31)$$

$$= \frac{kW}{2\pi}[\Theta(p + k_W/2) - \Theta(p - k_W/2)] \quad (32)$$

$$\approx \begin{cases} k/\beta(p), & p \neq \pm k \\ c_f(1-i)\sqrt{W/\lambda}, & p = \pm k \end{cases}, \quad (33)$$

$$c_f = 0.942, \quad (34)$$

where $\Theta(p \pm k_W/2)$ is defined by (9). When $W/\lambda > 10^3$, (33) becomes fairly accurate. When $p = \pm k$, however, (32) gives $(1-i)\sqrt{W/\lambda}$, which is slightly different in numerical values from the integral on the right hand side of (30). To correct this, we numerically determined the factor c_f in (34). Physically, $\Theta(p + nk_L + k_W/2) - \Theta(p + nk_L - k_W/2)$ is a (complex) beam width of the nth order diffraction beam scattered into the $\theta_s = \Theta(p + nk_L)$ direction. The lower equation of (33) implies that a diffraction beam scattered into a grazing direction has a much wider beam width proportional to $\sqrt{\lambda/W}$, whereas the upper equation means that a beam into a non-grazing direction has a narrow beam width proportional to λ/W.

Applying (28) and (29) to (26), we obtain for sufficiently large W,

$$D_{l,n}(p) = v_{l-n}(p + nk_L, \beta(p + nk_L))$$
$$+ \frac{\sigma k_L(p + nk_L)}{2k}\Delta(p + nk_L, W)[\delta_{n,l-1} + \delta_{n,l+1}]. \quad (35)$$

By (33), $D_{l,n}(p)$ is independent of W when $p + nk_L \neq \pm k$ but becomes proportional to $\sqrt{W/\lambda}$ when $p + nk_L = \pm k$.

2.3 Cramer's Solution

By Cramer's formula, the solution of (19) is written as $Q_n = \mathcal{E}_n(p)/\mathcal{D}(p)$, where $\mathcal{D}(p)$ and $\mathcal{E}_n(p)$ are determinants.

$$\mathcal{D}(p) =$$

$$\{0\} \begin{vmatrix} \overset{(-N_Q)}{D_{-N_Q,-N_Q}} & \cdots & \overset{(0)}{D_{-N_Q,0}} & \cdots & \overset{(N_Q)}{D_{-N_Q,N_Q}} \\ \cdot & \cdots & \cdot & \cdots & \cdot \\ \cdot & \cdots & \cdot & \cdots & \cdot \\ D_{0,-N_Q} & \cdots & D_{0,0} & \cdots & D_{0,N_Q} \\ \cdot & \cdots & \cdot & \cdots & \cdot \\ \cdot & \cdots & \cdot & \cdots & \cdot \\ D_{N_Q,-N_Q} & \cdots & D_{N_Q,0} & \cdots & D_{N_Q,N_Q} \end{vmatrix}$$

$$= \sum_{m=-N_Q}^{N_Q} (-1)^m D_{m,0}(p) \mathcal{D}^{[m,0]}(p), \qquad (36)$$

$$\mathcal{E}_n(p) =$$

$$\{0\} \begin{vmatrix} \overset{(-N_Q)}{D_{-N_Q,-N_Q}} & \cdots & \overset{(n)}{E_{-N_Q}} & \cdots & \overset{(N_Q)}{D_{-N_Q,N_Q}} \\ \cdot & \cdots & \cdot & \cdots & \cdot \\ \cdot & \cdots & \cdot & \cdots & \cdot \\ D_{0,-N_Q} & \cdots & E_0 & \cdots & D_{0,N_Q} \\ \cdot & \cdots & \cdot & \cdots & \cdot \\ \cdot & \cdots & \cdot & \cdots & \cdot \\ D_{N_Q,-N_Q} & \cdots & E_{N_Q} & \cdots & D_{N_Q,N_Q} \end{vmatrix}$$

$$= \sum_{m=-N_Q}^{N_Q} (-1)^{m+n} E_m(p) \mathcal{D}^{[m,n]}(p) \qquad (37)$$

$$= \sum_{m=-N_Q}^{N_Q} (-1)^m D_{m,0}(p) \mathcal{E}_n^{[m,0]}(p), \qquad (38)$$

where $\{0\}$ stands for the 0th row and (n) the nth column. In these determinants, p is omitted. By the notation $\mathcal{D}^{[m,n]}(p)$, for example, we mean the determinant obtained from $\mathcal{D}(p)$ by eliminating the mth row and nth column. However, there are many expressions for the determinant $\mathcal{E}_n(p)$. For example, $\mathcal{E}_n(p)$ is unchanged by adding the nth column vector multiplied by a constant μ to the 0th column vector. In other words, if $n \neq 0$, we may replace the 0th column vector $[D_{-N_Q,0}(p), \cdots, D_{0,0}(p), \cdots, D_{N_Q,0}(p)]^t$ by $[D_{-N_Q,0}(p) + \mu E_{-N_Q}(p), \cdots, D_{0,0}(p) + \mu E_0(p), \cdots, D_{N_Q,0}(p) + \mu E_{N_Q}(p)]^t$, t denoting the transpose. Thus, we have from (38),

$$\mathcal{E}_n(p) = \sum_{m=-N_Q}^{N_Q} (-1)^m [D_{m,0}(p) + \mu E_m(p)] \mathcal{E}_n^{[m,0]}(p),$$

$$(n \neq 0). \qquad (39)$$

where μ is any constant.

Using Cramer's rule, (36) and (37), we may obtain the solution Q_0 as

$$Q_0 = \frac{\mathcal{E}_0(p)}{\mathcal{D}(p)} = \frac{\displaystyle\sum_{m=-N_Q}^{N_Q} (-1)^m E_m(p) \mathcal{D}^{[m,0]}(p)}{\displaystyle\sum_{m=-N_Q}^{N_Q} (-1)^m D_{m,0}(p) \mathcal{D}^{[m,0]}(p)}. \qquad (40)$$

Using (36) and (39), we also obtain the solution Q_n as

$$Q_n = \frac{\displaystyle\sum_{m=-N_Q}^{N_Q} (-1)^m [D_{m,0}(p) + \mu E_m(p)] \mathcal{E}_n^{[m,0]}(p)}{\displaystyle\sum_{m=-N_Q}^{N_Q} (-1)^m D_{m,0}(p) \mathcal{D}^{[m,0]}(p)},$$

$$(n \neq 0). \qquad (41)$$

Using these formulas, we next obtain asymptotic formulas for Q_0 and Q_n.

3. Asymptotic Solution at LGLI

Let us calculate Q_n at LGLI. In what follows, however, we implicitly assume the single anomaly case, where $k + nk_L \neq -k$ holds for any integer n. Putting $p = k$, $\beta(p) = 0$, and $n = 0$ in (35) and using (24), we obtain

$$D_{m,0}(k) \approx \begin{cases} 1, & m = 0 \\ \dfrac{\sigma k_L}{2} \Delta(k, W), & m = \pm 1 \\ 0, & |m| = 2, 3, 4, \cdots \end{cases} \qquad (42)$$

By (33), we have

$$\frac{\sigma k_L}{2} \Delta(k, W) = \frac{(1-i)c_f}{2} \left(\frac{2\pi\sigma}{L} \right) \sqrt{\frac{W}{\lambda}}, \qquad (43)$$

which is proportional to the Rayleigh slope parameter $2\pi\sigma/L$ and $\sqrt{W/\lambda}$. In the single anomaly case, only $D_{\pm 1,0}(k)$ increases proportional to $\sqrt{W/\lambda}$ but any other component $D_{m,n}(p)$ is independent of W. From (21) and (25), we have

$$E_m(k) = -\sigma k k_L (\delta_{m,1} + \delta_{m,-1}). \qquad (44)$$

To calculate the numerator of (41), we put $\mu = \Delta(k, W)/(2k)$. Then, we have from (42) and (44),

$$D_{m,0}(k) + \frac{\Delta(k, W)}{2k} E_m(p) = \delta_{m,0}. \qquad (45)$$

Applying this relation to (41), we obtain

$$Q_n = \frac{\mathcal{E}_n^{[0,0]}(k)}{\mathcal{D}^{[0,0]}(k) - \dfrac{\sigma k_L}{2} \Delta(k, W)[\mathcal{D}^{[-1,0]}(k) + \mathcal{D}^{[1,0]}(k)]}. \qquad (46)$$

In the single anomaly case, $\mathcal{D}^{[0,0]}(k)$, $\mathcal{D}^{[-1,0]}(k)$, $\mathcal{D}^{[1,0]}(k)$ and $\mathcal{E}_n^{[0,0]}(k)$ are all independent of W. But they depend on L and σ. Since $\sigma k_L \Delta(k, W)/2$ in (46) diverges by (43) when $W \to \infty$, we obtain the asymptotic expression of Q_n as

$$Q_n = -\frac{\mathcal{E}_n^{[0,0]}(k)}{[\mathcal{D}^{[-1,0]}(k) + \mathcal{D}^{[1,0]}(k)]} \frac{2}{\sigma k_L \Delta(k, W)} \qquad (47)$$

$$= -\frac{\mathcal{E}_n^{[0,0]}(k)}{[\mathcal{D}^{[-1,0]}(k) + \mathcal{D}^{[1,0]}(k)]} \frac{2}{\sigma k_L c_f (1-i)} \sqrt{\frac{\lambda}{W}}, \qquad (48)$$

where $n \neq 0$. Since $\mathcal{E}_n^{[0,0]}(k)$ is proportional to $\sigma k k_L$ by (44), (48) remains finite even at $\sigma \to 0$. However, it is difficult

to obtain a concrete expression of Q_n ($n \neq 0$), because analytical expressions for $\mathcal{E}_n^{[0,0]}(k)$ and $\mathcal{D}^{[\pm 1,0]}(k)$ are difficult to obtain.

Next, we substitute (42) and (44) into (40) to obtain,

$$Q_0 = \frac{\sigma k k_L [\mathcal{D}^{[-1,0]}(k) + \mathcal{D}^{[1,0]}(k)]}{\mathcal{D}^{[0,0]}(k) - \frac{\sigma k_L}{2}\Delta(k,W)[\mathcal{D}^{[-1,0]}(k) + \mathcal{D}^{[1,0]}(k)]}. \tag{49}$$

Since $\Delta(k,W)$ diverges as $W \to \infty$, we obtain the asymptotic expression of Q_0 as

$$Q_0 = -\frac{2k}{\Delta(k,W)} = -\frac{(1+i)k}{c_f}\sqrt{\frac{\lambda}{W}}. \tag{50}$$

Here, (48) and (50) mean that Q_n decreases proportional to $\sqrt{\lambda/W}$ for sufficiently large W. Furthermore, Q_0 in (50) is independent of L and σ. These properties should be understood as multiple scattering effects[†]. However, the convergence from (46) to (48) and from (49) to (50) is expected to be slow, because $\Delta(k,W)$ is proportional to $\sqrt{W/\lambda}$. Furthermore, (43) suggests that the convergence could become much slow, when the surface slope $2\pi\sigma/L$ is small. It can be shown after some manipulation that $[\mathcal{D}^{[-1,0]}(k) + \mathcal{D}^{[1,0]}(k)]/\mathcal{D}^{[0,0]}(k)$ is proportional to σ. Thus, when σ is small, the convergence becomes much slow. These properties will be seen in numerical examples below.

3.1 Total Scattering Cross Section at LGLI

In the finite periodic case, the scattered wave becomes a sum of diffraction beams, of which the main lobes are scattered into the $\Theta(p + nk_L)$ ($n = 0, \pm 1, \pm 2, \cdots$) directions. Thus, the differential scattering cross section has a peak value $\sigma_s(\Theta(p + nk_L)|\theta_i)$ and a (real) beam width $Re[\Theta(p + nk_L + k_W/2) - \Theta(p + nk_L - k_W/2)]$. Taking these facts and (13), we roughly obtain

$$\frac{p_{inc}}{\lambda} = \frac{W}{2\pi\lambda}\sum_n \sigma_s(\Theta(p + nk_L)|\theta_i)Re[\Theta(p + nk_L + k_W/2) - \Theta(p + nk_L - k_W/2)]. \tag{51}$$

Putting $\theta_i = 0$ and $p = k$, let us evaluate the right-hand side. Substituting (15) into (14) and using (48) and an approximate relation $U(s - nk_L|W)U(s - mk_L|W) \approx 0$ for $n \neq m$, we obtain

$$\sigma_s(\Theta(k + nk_L)|0) \approx \frac{W}{k}|Q_n|^2$$
$$= 4\pi\left|\frac{\mathcal{E}_n^{[0,0]}(k)}{[\mathcal{D}^{[-1,0]}(k) + \mathcal{D}^{[1,0]}(k)]}\frac{1}{\sigma k_L c_f}\right|^2, \quad (n \neq 0), \tag{52}$$

which is independent of W. We also obtain for $n = 0$ as

$$\sigma_s(\Theta(k)|0) \approx \frac{W}{k}|Q_0|^2 = \frac{4\pi}{c_f^2} = 14.162 \ (11.52\,\text{dB}), \tag{53}$$

which means $\sigma_s(\pi|0) = \sigma_s(\Theta(k)|0)$ does not depend on L, σ

and W, if W is sufficiently large. Using (32) and (33), we obtain

$$\frac{p_{inc}}{\lambda} = \sum_{n\neq 0}\sigma_s(\Theta(k + nk_L)|0)Re\left[\frac{1}{\lambda\beta(k + nk_L)}\right]$$
$$+ \sigma_s(\Theta(k)|0)\frac{c_f}{2\pi}\sqrt{\frac{W}{\lambda}}. \tag{54}$$

Since $\sigma_s(\Theta(k + nk_L)|0)$ is independent of W for any n, we obtain a new asymptotic formula for sufficiently large W as

$$\frac{p_{inc}}{\lambda} = \frac{2}{c_f}\sqrt{\frac{W}{\lambda}}. \tag{55}$$

Next, let us calculate p_c. By (15) and (17), we may write the total scattering cross section p_c as,

$$p_c = -\frac{4\pi}{k}Re[A_\beta(0)] = -2\frac{W}{k}Re[Q_0]. \tag{56}$$

From (50) and (56), we obtain a new asymptotic solution for sufficiently large W as

$$\frac{p_c}{\lambda} = \frac{2}{c_f}\sqrt{\frac{W}{\lambda}}. \tag{57}$$

Here, it is important to note that the optical theorem (11) holds by (57) and (55).

By (57) we obtain the scattering cross section per unit surface p_c/W for sufficiently large W as

$$\frac{p_c}{W} = \frac{2}{c_f}\sqrt{\frac{\lambda}{W}}. \tag{58}$$

Formulas (57), (55) and (58) are important results of this paper. The equations (57) and (55) mean that the total scattering cross section does not depend on the surface roughness σ and the period L. This implies that the scattering becomes quite singular at LGLI, when W is sufficiently large. When $W \to \infty$, however, the total scattering cross section p_c at LGLI diverges and hence has no physical significance. In other words, the scattering is defined only for a target with finite extent. However, p_c/W the total scattering cross section per unit surface can be defined even when $W \to \infty$. The equation (58) means that p_c/W vanishes as $W \to \infty$. This means physically that the diffraction by a periodic surface with infinite extent does not occur at LGLI. This agrees with theoretical and numerical results on the diffraction by periodic gratings [2]–[7].

However, it can be shown theoretically (50) and (57) are valid even in the double anomaly case where $k + nk_L = -k$ holds for a certain integer n.

[†]In a case where σ is sufficiently small and W is not large, the factor $\sigma k_L\Delta(k,W)/2$ and the second term in the denominator in (49) become small. As a result, we obtain a single scattering approximation as $Q_0 = \sigma k k_L[\mathcal{D}^{[-1,0]}(k) + \mathcal{D}^{[1,0]}(k)]/\mathcal{D}^{[0,0]}(k)$, which is independent of W. In this case, p_c becomes linearly proportional to W by (56). However, we will obtain an explicit expression of the total scattering cross section (59) by the small perturbation method.

4. Comparison with Numerical Results

We have obtained a new analytic formula of the total scattering cross section (57) at LGLI. We also obtain an analytical expression for the differential scattering cross section $\sigma_s(\theta_s|\theta_i)$ at $\theta_s = \pi$ and $\theta_i = 0$. To see their validity, let us compare with some numerical results.

In the numerical examples below, we put $N_Q = 7$ and $k_B = (N_Q + 1/2)k_L$. We set $\theta_i = 0.00001°$ instead of $\theta_i = 0$. Then, we numerically calculated the integral in (20) and then we solved (19) numerically to obtain the total scattering cross section p_c.

4.1 Example 1

To consider a single anomaly case, we put the period as $L = 2.75\lambda$. Then, we obtain the total scattering cross section p_c at $\theta_i = 0.00001°$ for $\sigma/\lambda = 0.2$, 0.3 and 0.4 and for $W/\lambda = 1760$, 3520, 7040, 14080 and 28160, where the error with respect to the optical theorem is always less than 3.4×10^{-4}. The result is plotted against W/λ in Fig. 2, where the theoretical value by (57) is also plotted. As is expected above, the numerical result becomes close to the theoretical value when σ/λ and W/λ become large. Note that the dependence of p_c/λ on σ/λ becomes small when W/λ becomes large.

Let us see some numerical examples. When $W/\lambda = 1760$, we have $p_c/\lambda = 98.71$, 93.70 and 91.17 at $\sigma/\lambda = 0.2$, 0.3 and 0.4, respectively, whereas the theoretical value by (57) is 89.07. When $W/\lambda = 28160$, we find $p_c/\lambda = 369.56$, 361.55 and 358.48 at $\sigma/\lambda = 0.2$, 0.3 and 0.4, respectively, which are close to the theoretical value 356.48. Disagreements between numerical calculations and the theoretical values by (57) are 3.7%, 1.4% and 0.4% at $\sigma/\lambda = 0.2$, 0.3 and 0.4, respectively, when $W/\lambda = 28160$. The disagreement becomes larger as σ becomes smaller, because

the convergence from (49) to (50) becomes slower. However, we may conclude (57) is fairly accurate when W/λ becomes large enough.

Let us see the differential scattering cross section $\sigma_s(\theta_s|\theta_i)$ at $\theta_i = 0.00001°$ and $\theta_s = 180°$. By numerical calculations, $\sigma_s(180°|\,0.00001°)$ becomes 10.98 dB, 11.20 dB and 11.22 dB at $\sigma/\lambda = 0.2$, 0.3 and 0.4, respectively, when $W/\lambda = 1760$. When $W/\lambda = 28160$, however, $\sigma_s(180°|\,0.00001°)$ becomes 11.40 dB, 11.43 dB and 11.43 dB at $\sigma/\lambda = 0.2$, 0.3 and 0.4, respectively. These values are much closer to the theoretical estimation 11.52 dB in (53).

4.2 Example 2

We put $L = 2.5\lambda$ to see a double anomaly case. We also calculated p_c at $\theta_i = 0.00001°$ for $\sigma/\lambda = 0.2$, 0.3 and 0.4, and for $W/\lambda = 1600$, 3200, 6400, 12800 and 25600, for which the error with respect to the optical theorem is always less than 7×10^{-4}. Then, we plotted p_c against W/λ in Fig. 3. We see in the figure that the numerical result becomes close to the theoretical value when σ/λ and W/λ become large. We also see that the dependence of p_c/λ on σ/λ becomes small when W/λ becomes large.

When $W/\lambda = 1600$, we have $p_c/\lambda = 93.36$, 88.86 and 86.64 at $\sigma/\lambda = 0.2$, 0.3 and 0.4, respectively, whereas (57) gives 84.92. When $W/\lambda = 25600$, we have $p_c/\lambda = 351.01$, 344.12 and 341.47 at $\sigma/\lambda = 0.2$, 0.3 and 0.4, respectively, which is much close to the theoretical value 339.70. In fact, disagreements are 3.3%, 1.3% and 0.5% at $\sigma/\lambda = 0.2$, 0.3 and 0.4, respectively, when $W/\lambda = 25600$. Here, we see again that the disagreement becomes larger as σ becomes smaller. However, this example implies that (57) is applicable to a double anomaly case.

Next, let us see $\sigma_s(\theta_s|\theta_i)$ at $\theta_i = 0.00001°$ and $\theta_s = 180°$. When $W/\lambda = 1600$, we found numerically that $\sigma_s(180°|\,0.00001°)$ becomes 11.02 dB, 11.20 dB and 11.22 dB at $\sigma/\lambda = 0.2$, 0.3 and 0.4, respectively.

Fig. 2 Total scattering cross section p_c/λ against the corrugation width W/λ. $L = 2.75\lambda$, $\theta_i = 0.00001°$. 'ASYM' indicates the asymptotic solution (57).
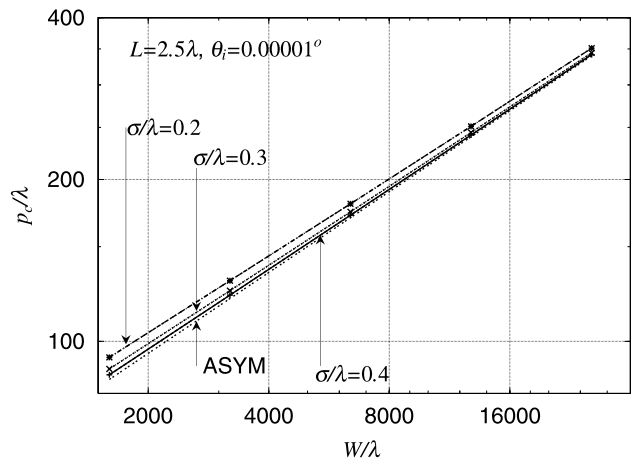
Fig. 3 Total scattering cross section p_c/λ against the corrugation width W/λ. $L = 2.5\lambda$, $\theta_i = 0.00001°$. 'ASYM' indicates the asymptotic solution (57).

When $W/\lambda = 25600$, however, $\sigma_s(180°|\,0.00001°)$ becomes 11.40 dB, 11.43 dB and 11.43 dB at $\sigma/\lambda = 0.2$, 0.3 and 0.4, respectively. These values are much close to the theoretical value 11.52 dB in (53). Therefore, we may conclude again that our estimation of (53) is fairly accurate if W is large enough.

5. Discussions

In order to obtain the asymptotic behavior of p_c at LGLI, our discussions have been restricted to a sufficiently large W case.

Now let us consider a case where W is not large and σ is much smaller than the wavelength. In such a case, the single scattering process is dominant and the scattered wave may be described by the first order perturbation [13]. The total scattering cross section $p_c^{(2)}$ may be given by the second order perturbation as[†]

$$\frac{p_c^{(2)}}{\lambda} \approx \frac{W}{\lambda}\left(\frac{2\pi\sigma}{L}\right)^2 \frac{k}{\beta(k - k_L)}, \qquad (59)$$

which is entirely different from the asymptotic solution (57). Clearly, $p_c^{(2)}$ depends on the Rayleigh slope parameter $2\pi\sigma/L$ and is proportional to W, whereas the asymptotic solution (57) is proportional to $\sqrt{W/\lambda}$ and is independent of L and σ. This suggests that the W region is divided into two regions: the single scattering region where (59) is valid and the multiple scattering region where (57) is useful. The transition point W_t between these regions is determined from (57) and (59) as

$$\frac{W_t}{\lambda} = \left[\frac{2}{c_f}\frac{\beta(k - k_L)}{k}\right]^2 \left(\frac{2\pi\sigma}{L}\right)^{-4}, \qquad (60)$$

which depends on σ/λ and L/λ. However, we note that (59) and (60) hold only for a sinusoidal case.

To see these regions, we numerically calculated p_c for $\theta_i = 0.00001°$, $L = 2.5\lambda$ and $\sigma = 0.1\lambda$ and for W/λ from 50 to 25600. The result is shown in Fig. 4, where two straight lines indicate theoretical estimations by (59) and (57). The lines intersect at the transition point $W = W_t = 723\lambda$. Figure 4 clearly shows that p_c/λ by numerical calculations is linearly proportional to W/λ if $W \leq 200\lambda$ and becomes almost proportional to $\sqrt{W/\lambda}$ when $W \geq 6400\lambda$. This means that the W region is divided into the single and multiple scattering regions. In other words, the perturbation solution (59) is applicable in the single scattering region with $W \ll W_t$. On the other hand, our asymptotic solution (57) is useful in the multiple scattering region with $W \gg W_t$. This is an important conclusion of this paper[††] .

[†]Here, we implicitly assume $|k - k_L| < k$. Equation (59) may be obtained from (24) in Ref. [13] by putting $p = k$.

[††]In the case of Fig. 4, $p_c^{(2)}/\lambda$ by (59) is about 10% smaller than the numerical solution when $W = 50\lambda$. Also, p_c/λ by (57) is 15% (12%) smaller than the numerical solution at $W/\lambda = 6400$ ($W/\lambda = 25600$).
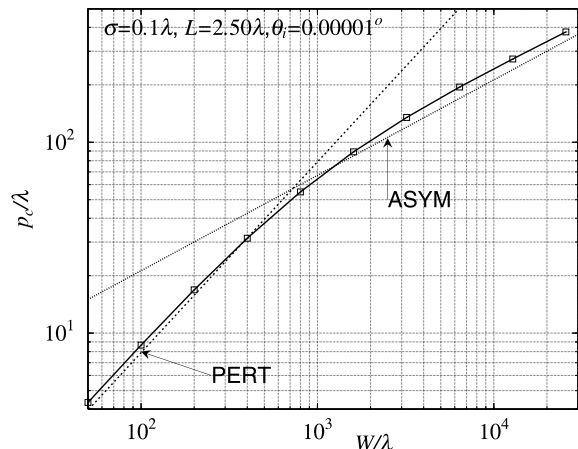
Fig. 4 Total scattering cross section p_c/λ against the corrugation width W/λ. $\sigma = 0.1\lambda$, $L = 2.5\lambda$, and $\theta_i = 0.00001°$. A box indicates the numerical solution. 'PERT' and 'ASYM' indicate the theoretical estimations by the second order perturbation (59) and by the asymptotic solution (57), respectively. These theoretical lines intersect at the transition point $W = W_t = 723\lambda$.

6. Conclusions

This paper deals with the scattering of a TM plane wave from a perfectly conductive sinusoidal surface with finite extent. In general, numerical methods are required to obtain properties of the scattering. By use of the undersampling approximation and a rectangular approximation, however, we successfully obtain a new analytical formula for the total scattering cross section at a low grazing limit of incident angle for a large corrugation width. The asymptotic formula (57) represents a remarkable fact that the total scattering cross section is independent of the period and the surface roughness and increases in proportion to the square root of the corrugation width. By comparison with numerical results, we found that the formula is fairly accurate, when the surface is small in roughness and in slope, and when the corrugation width W is large enough. We newly introduced the transition point W_t between the single and multiple scattering regions. Then, we conclude that the asymptotic formula becomes useful in the multiple scattering region where the corrugation width W is much larger than the transition point W_t.

Our discussions were restricted to a special case where the surface is sinusoidal, the angle of incidence is low grazing and the corrugation width is sufficiently large. It is important to derive a formula applicable to any angle of incidence for a non-sinusoidal surface. Moreover, we are interested in obtaining an analytic expression of the backscattering cross section for the remote sensing application. However, these problems are left for future study.

References

[1] D.E. Barrick, "Grazing behavior of scatter and propagation above any rough surface," IEEE Trans. Antennas Propag., vol.46, no.1,

pp.73–83, Jan. 1998.

[2] M.I. Charnotskii, "Wave scattering by periodic surface at low grazing angles: Single grazing mode," Progress in Electromagnetic Research, PIER 26, pp.1–42, 2000.

[3] J. Nakayama, K. Hattori, and Y. Tamura, "Diffraction amplitudes from periodic Neumann surface: Low grazing limit of incidence," IEICE Trans. Electron., vol.E89-C, no.5, pp.642–644, May 2006.

[4] J. Nakayama, K. Hattori, and Y. Tamura, "Diffraction amplitudes from periodic Neumann surface: Low grazing limit of incidence (II)," IEICE Trans. Electron., vol.E89-C, no.9, pp.1362–1364, Sept. 2006.

[5] H. Ikuno and K. Yasuura, "Improved point-matching method with application to scattering from a periodic surface," IEEE Trans. Antennas Propag., vol.AP-21, no.5, pp.657–662, May 1973.

[6] T. Yamasaki and T. Hinata, "Scattering of electromagnetic wave by plane grating with reflector," IECE Trans. Commun. (Japanese Edition), vol.J61-B, no.11, pp.935–942, Nov. 1978.

[7] J. Yamakita and K. Rokushima, "Scattering of plane waves from dielectric gratings with deep grooves," IECE Trans. Commun. (Japanese Edition), vol.J66-B, no.3, pp.375–382, March 1983.

[8] V.I. Tatarski and M. Charnotskii, "Universal behavior of scattering amplitude for scattering from a plane in average rough surface for small grazing angles," Waves Random Media, vol.8, no.1, pp.29–40, 1998.

[9] A. Kashihara and J. Nakayama, "Scattering of TM plane wave from a finite periodic surface," IEICE Trans. Electron. (Japanese Edition), vol.J88-C, no.7, pp.493–501, July 2005.

[10] J. Nakayama and Y. Tamura, "Scattering of a TM wave from a periodic surface with finite extent: Undersampling approximation," IEICE Trans. Electron., vol.E90-C, no.2, pp.304–311, Feb. 2007.

[11] J. Nakayama and Y. Tamura, "Low grazing scattering from sinusoidal Neumann surface with finite extent: Undersampling approximation," IEICE Trans. Electron., vol.E91-C, no.1, pp.9–16, Jan. 2008.

[12] J. Nakayama, K. Hattori, and Y. Tamura, "Low grazing scattering from periodic Neumann surface with finite extent," IEICE Trans. Electron., vol.E90-C, no.4, pp.903–906, April 2007.

[13] J. Nakayama, Y. Ochi, and Y. Tamura, "Scattering of a TM plane wave from a periodic surface with finite extent: Perturbation solution," IEICE Trans. Electron., vol.E89-C, no.9, pp.1358–1361, Sept. 2006.

[14] R. Petit, ed., Electromagnetic theory of gratings, Springer, Berlin, 1980.
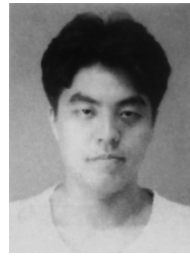
Yasuhiko Tamura received the B.E., M.E. and Ph.D. degrees from Kyoto Institute of Technology in 1991, 1993 and 2005, respectively. From 1993 to 1994 he worked in the Technical Research Institute, Konami Co., Ltd., Kobe. In 1994, he joined the staff of the Faculty of Engineering and Design, Kyoto Institute of Technology, where he is currently an Assistant Professor of the Graduate School of Engineering and Design. His research interests are electromagnetic wave theory, computational methods for stochastic analysis and visualization for electromagnetic field. Dr. Tamura received the Paper Presentation Award from Institute of Electrical Engineering of Japan in 1996.

Junichi Nakayama received the B.E. degree from Kyoto Institute of Technology in 1968, M.E. and Dr. Eng. degrees from Kyoto University in 1971 and 1982, respectively. From 1971 to 1975 he worked in the Radio Communication Division of Research Laboratories, Oki Electric Industry, Tokyo. In 1975, he joined the staff of the Faculty of Engineering and Design, Kyoto Institute of Technology, where he is currently a Professor of Electronics. From 1983 to 1984 he was a visiting research associate in the Department of Electrical Engineering, University of Toronto, Canada. Since 2002, he has been an editorial board member of *Waves in Random and Complex Media*. His research interests are electromagnetic wave theory, acoustical imaging and signal processing. Dr. Nakayama is a member of IEEE and a fellow of the Institute of Physics.